H. A. Davies, C. L. Harland, J. I. Betancourt R., Z. C. Wang
Department of Engineering Materials, University of Sheffield, United Kingdom

RECENT PROGRESS IN THE DEVELOPMENT OF NANOPHASE RARE EARTH MAGNETS

ABSTRACT

Nanocrystalline melt-spun rare earth – iron – boron alloys based on Pr and on Nd-Pr mixtures have been studied. Their magnetic properties are compared with those of corresponding alloy ribbons based on Nd. The Pr containing alloys have generally higher coercivity than their Nd counterparts because of the higher anisotropy constant of the $Pr_2Fe_{14}B$ phase. Co substitution for Fe increases the Curie temperature for both the Pr and Nd-Pr nanophase alloys. excellent magnetic property combinations were achieved for single phase $Pr_{12}(Fe_{100-x}Co_x)_{82}B_6$ (x = 0 – 20) alloys, processed by overquenching and devitrification annealing. Addition of 1 at % Zr as a grain refiner resulted in increased coercivity and maximum energy product of NdPrFeB alloys for the whole range of RE contents studied (8 – 12 at %).

INTRODUCTION

Rapid solidification technology has achieved perhaps its greatest commercial success in its application to both soft and hard magnetic alloys. Such alloys are of prime importance in many areas of technology including electricity generation and distribution, telecommunications, computer hardware, transport and consumer goods.

A major processing route for rare earth-iron-boron magnets is rapid solidification by chill block melt spinning to thin (~30 μm) ribbon, followed by crushing to powder and either pressure moulding with a polymer binder to form a bonded magnet [1] or hot pressing/extrusion to produce a fully dense magnet [2]. The bonding route is especially attractive because of the shape flexibility that it offers for magnets and of its adaptability to integrated manufacture.

Although this ribbon material has a very high coercivity ${}_iH_c$, resulting from the microcrystalline structure (mean grain size d_g 60 – 100nm) [1], its maximum energy product $(BH)_{max}$ is limited by the fact that the uniaxial crystallites of the intermetallic compound $Nd_2Fe_{14}B$ are randomly oriented and that, in this range of diameters, they effectively behave as non-interacting magnetic particles. For such material, the remanent magnetisation J_r is restricted to a value of $0.5J_s$, where J_s is the saturation magnetisation [3].

It has subsequently been demonstrated, however, that, if d_g for the $Nd_2Fe_{14}B$ grains is reduced below~50nm, by careful process control, they interact with each other, as a result of a quantum mechanical phenomenon known as 'ferromagnetic exchange coupling'. The effect is to enhance J_r above the nominal theoretical limit of $J_s/2$ [4,5]. Thus, $(BH)_{max}$ is markedly increased, typically by up to ~60% [5]. Further increases in J_r and $(BH)_{max}$, have been obtained for off-stoichiometric, Fe-rich, alloys, which results in a *nanocomposite* structure containing grains of magnetically soft α-Fe phase, in addition to the hard $Nd_2Fe_{14}B$ crystallites [6, 7]. Thus, the soft grains, which have larger J_s than the $Nd_2Fe_{14}B$ phase (2.2T vs 1.6T), couple in completely to neighbouring hard phase grains and increase the exchange enhancement [8]. Similar behaviour has been reported for $Nd_2Fe_{14}B/Fe_3B$ [9] and $Sm_2Fe_{17}N_x/\alpha$-Fe [10] nanocomposite alloys.

This paper reviews some of the recent research undertaken in our laboratory at Sheffield on nanophase Rare Earth-Iron-Boron alloys. In particular, (i) Pr-Fe-B and mixed rare earth Nd/Pr-Fe-B variants, which yield higher ${}_iH_c$ than their Nd counterparts because of the increased anisotropy constant of the $RE_2Fe_{14}B$ phase [11-15]; (ii) attempts to obtain magnetic properties, by overquenching and annealing, equivalent to those that derive from direct quenching, in order to broaden the process window for improved commercial viability [12,14,16], (iii) the influence of alloying additions such as Co and Zr, to improve the thermal stability and the ${}_iH_c/(BH)_{max}$ combinations [14,15,16], are discussed.

EXPERIMENTAL

The procedures for preparation of alloys and for single roll melt spinning to thin ribbon have been described elsewhere [12]. The magnitude of grains in the ribbon is governed by the cooling rate and the resulting degree of undercooling of the melt during solidification, which are in turn controlled by the ribbon thickness and hence by the roll velocity and the melt flow rate through the orifice in the quartz nozzle. The spinning was performed in sealed argon at pressure of 0.25 atmosphere to minimise oxidation and to avoid the formation of gas pockets on the roll-contact surface of the solidified ribbon. Such pockets would lead to localised regions of lower cooling rate and thus to larger grains [17]. J-H loops, the important magnetic parameters J_r and ${}_iH_c$ and the derivative $(BH)_{max}$ were determined using single sample lengths of ribbon, typically 5-10 mm long with a VSM coupled to a 5 Tesla superconducting magnet. Measurements were made in-plane to avoid corrections for self demagnetising fields. Typically, six ribbon samples were measured separately and mean values of the properties determined. The value of d_g, usually for the $RE_2Fe_{14}B$ phase, but in some cases also for the soft magnetic bcc Fe-based phase, were determined by x-ray diffraction line broadening analysis, using the Scherrer formula and with averaging over several diffraction peaks [18].

INFLUENCE OF RE: FE RATIO AND GRAIN SIZE ON THE MAGNETIC PROPERTIES OF Nd-Fe-B, Pr-Fe-B AND Nd/Pr-Fe-B ALLOYS

The effects of the RE concentrations on J_r, ${}_iH_c$ and $(BH)_{max}$ for $Nd_yFe_{94-y}B_6$, $Pr_yFe_{94-y}B_6$ and $(Nd_{0.75}Pr_{0.25})_yFe_{94-y}B_6$ alloys for approximately constant mean $RE_2Fe_{14}B$ grain size d_g, lying in the range 20-35 nm, are shown in Fig. 1.The ranges of y covered are 8-19, 6-20 and 8-14 for the Nd, Pr and Nd/Pr series, respectively.

The trends of J_r for the three systems are very similar in the range of compositional overlap, the slightly larger values being associated with the PrFeB system, probably because of d_g being systematically the smallest for this alloy series. However, notwithstanding the slightly smaller d_g, ${}_iH_c$ is clearly systematically higher for the PrFeB alloys. The relative difference, allowing for experimental scatter, averages 20-30%; the absolute difference increases with increasing y to a maximum of ~480 kA/m at 14% RE. The difference in ${}_iH_c$ over the range 8-14 at % RE is consistent with the 30% larger value of H_A for the $Pr_2Fe_{14}B$ phase than its Nd counterpart at room temperature [19]. For RE concentrations greater than 14 at %, the difference in ${}_iH_c$ becomes progressively narrower, presumably because the coercivity becomes more dominated by the complex effects of the paramagnetic RE-rich phase in each case, and this is also the reason for the very steep increase in the magnitude of ${}_iH_c$ through the RE concentration range 12-16 at %.

The larger value of $_iH_c$ for the PrFeB series is especially important at low RE contents ≤ 10 at % where $_iH_c$ is reduced substantially because of the effect of the increasing volume fraction of soft magnetic α-Fe phase.

The Didymium-Fe-B series of alloys chosen in this case for the comparison of properties with the NdFeB and PrFeB series is based on the Nd:Pr ratio of 3:1 since this approximates to the relative proportions of the two metals that occur in rare earth ores. As would be expected on the basis of the similar magnitude of d_g, the J_r enhancement corresponds closely with those for the Nd and Pr series over the range of RE:Fe ratios that are in common for the three series. At the stoichiometric RE concentration (~12 at %), enhancement of J_r over the respective Stoner - Wohlfarth values [3] (0.8 T for $Nd_2Fe_{14}B$ and 0.79 T for $Pr_2Fe_{14}B$) is due entirely to

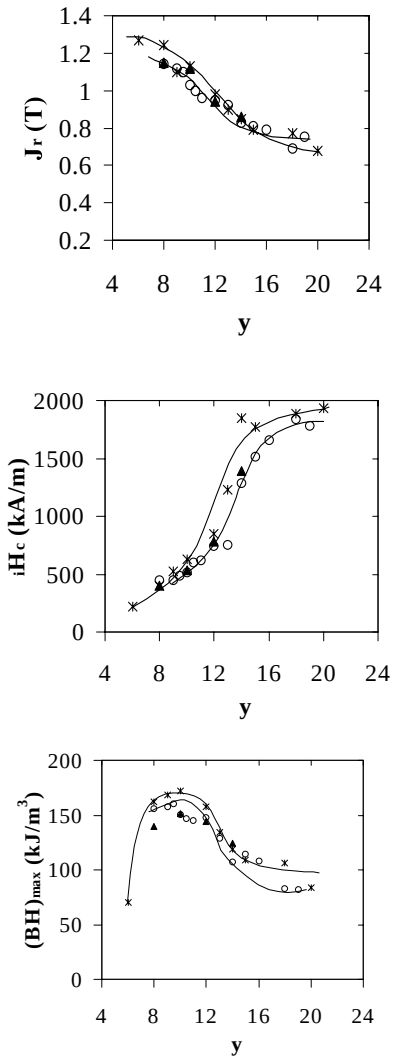

Fig. 1. Effects of RE concentration on the magnetic properties of nanophase $Nd_yFe_{94-y}B_6$ (o), $Pr_yFe_{94-y}B_6$ (s), and $(Nd_{0.75}Pr_{0.25})_yFe_{94-y}B_6$, (s) alloy ribbons with d_g for the $RE_2Fe_{14}B$ phase of ~ 25 30 nm, 20-30 nm and 25-32 nm, respectively

a significant degree of exchange coupling between the grains of 2/14/1 phase in each case [4,5]. The increasing J_r below 12 at % RE reflects a progressively increasing volume fraction of soft magnetic α-Fe nanocrystallites [6,8]. These have a larger saturation polarisation J_s [2.2 T] than the 2/14/1 phases (1.6 and 1.59 T for the Nd and Pr variants, respectively) and, since they have a mean diameter of approximately one half of d_g, they are completely exchange coupled with adjacent grains of 2/14/1 phase. It is, however, noticeable that the rate of increase of J_r with decreasing RE content tends to diminish below ~10 at % for all the series. The reason for this may be that, even though the volume fraction of the α-Fe is increasing, the reducing area of hard phase intergrain contact may be tending to decrease the effectiveness of the soft phase contributions in the remanent state.

$(BH)_{max}$, on initially decreasing the RE content below 12 at %, increases more sharply than J_r, as would be expected from the very approximate relation $(BH)_{max} \alpha (J_r)^2$ but this is not maintained below ~11 at % RE and, in fact, it tends to peak at ~9-10 at % RE because of the rapidly diminishing ${}_iH_c$, However, the fact that ${}_iH_c$ is significantly larger for PrFeB alloys than their Nd counterparts probably contributes to the larger $(BH)_{max}$ in the range 9-10 at % RE, in addition to the effect of a slightly larger J_r. The drastic effect of the diminishing ${}_iH_c$ on $(BH)_{max}$, through its influence in giving a non-linear second quadrant B-H characteristic, is seen in particular for the PrFeB alloys, for which the measurements were extended down to 6 at % RE. In this composition range, $(BH)_{max}$ drops catastrophically to a level similar to that typical of $Fe_{77}Nd_{4.5}B_{18.5}$ [9] which contains a very large volume fraction of soft phase, in this case Fe_3B. The latter, in fact, does not manifest enhancement of $(BH)_{max}$ above the value for non-exchange coupled, single phase $Nd_2Fe_{14}B$, in spite of a smaller d_g than for the $RE_2Fe_{14}B$/α-Fe alloy type being discussed in the present paper. Thus, the most useful composition ranges with respect to enhanced $(BH)_{max}$ and acceptable ${}_iH_c$, bearing in mind the higher raw material costs than for the $RE_2Fe_{14}B/Fe_3B$ type of nanocomposite alloys, are probably ~10-13 at % and ~8-13 at % RE for the NdFeB and PrFeB alloy series, respectively.

INFLUENCE OF CRYSTALLITE SIZE ON THE MAGNETIC PROPERTIES OF NANOCOMPOSITE ALLOYS

The observed effects of decreasing mean $RE_2Fe_{14}B$ grain size d_g on J_r and ${}_iH_c$ for a single phase alloy are well documented [5] and the results of micromagnetic computations are in good agreement with the experimental data for the stoichiometric $Nd_2Fe_{14}B$ alloy [20]. The influence of d_g on the properties of corresponding nanocomposite alloys does not, however, appear to have been subjected to systematic experimental study. It was observed earlier [21] that both J_r and ${}_iH_c$ increased as d_g was decreased for a sub-stoichiometric NdFeB alloys containing 9 at % Nd and this trend has also been predicted from micromagnetic modelling, with the enhancement of ${}_iH_c$ becoming more pronounced with increasing volume fraction of α-Fe, i.e. decreasing RE content [22].

The dependences of J_r and ${}_iH_c$ on d_g for two nanocomposite Didymium-Fe-B alloys, of compositions $(Nd_{0.75}Pr_{0.25})_{10}Fe_{84}B_6$ and $(Nd_{0.75}Pr_{0.25})_8Fe_{84}B_6$ and containing, respectively, about 15 and 30 vol % of α-Fe phase, are shown in Fig. 2. In both cases J_r, as expected, increases with decreasing d_g below ~40 nm, reflecting the increasing degree of exchange coupling. For the 10 at % RE alloy, ${}_iH_c$ decreases slightly for d_g below ~40 nm, indicating an intermediate case between the clear decrease for a single phase alloy [5] and the substantial increase predicted for large volume fractions of soft phase [22]. In contrast, the 8 at % RE alloy manifests a shallow increase of ${}_iH_c$ with decreasing d_g, albeit on a much lower absolute base value, consistent with

the larger volume fraction of α-Fe and in qualitative agreement with the micromagnetic predictions [22].

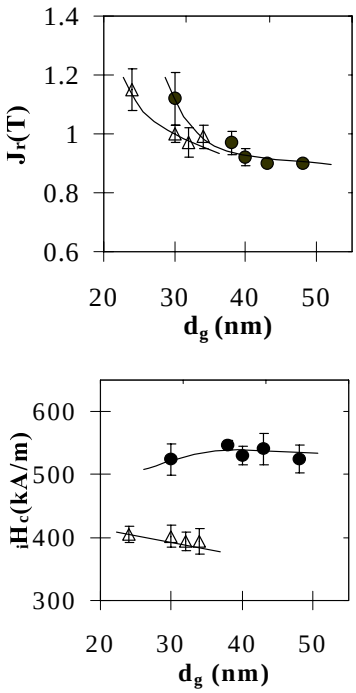

Fig. 2. Effects of decreasing mean grain diameter for the $RE_2Fe_{14}B$ phase on J_r and, $_iH_c$ for $(Nd_{0.75}Pr_{0.25})_{10}Fe_{84}B_6$ (ι) and $(Nd_{0.75}Pr_{0.25})_8Fe_{86}B_6$ (Δ)

PROPERTIES OF NANOPHASE DIDYMIUM-Fe-B ALLOYS WITH VARIABLE Nd:Pr RATIO

The effects of Pr substitutions for Nd on the magnetic properties of stoichiometric $(Nd_{1-x}Pr_x)_{12}Fe_{82}B_6$ alloys for an approximately constant d_g in the range 26-32 nm [13,14] are shown in Fig. 3. $_iH_c$ increases monotonically but at a progressively increasing rate between the Nd and Pr end points, reflecting the effect of Pr substitution into the 2/14/1 unit cell in enhancing H_A. The difference in $_iH_c$ between $Pr_{12}Fe_{82}B_6$ and $Nd_{12}Fe_{14}B_6$ is about 22%, which is roughly consistent with the difference in H_A between the two 2/14/1 phases [19]. The enhanced J_r is approximately constant at ~0.95 T, across most of the series, as would be expected for a nominally constant d_g and from the fact that J_s for $Pr_{12}Fe_{82}B_6$ is only some 1.3% smaller than for its Nd counterpart. The J_r enhancement is, however, significantly greater for x = 0.75 (at ~1.05 T). The reason for this is not clear; a possible explanation is that the ribbon samples used either for the magnetic property measurements or for the estimation of d_g were not representative of the whole sample. The higher J_r for x = 0.75 is also reflected in a substantially larger value of $(BH)_{max}$ of 180 kJm^{-3}, since $_iH_c$ for these stoichiometric nanophase alloys is relatively high. The $(BH)_{max}$-$_iH_c$ combination resulting from this 75% Pr substitution is excellent.

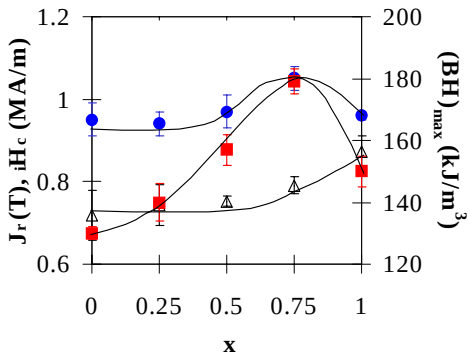

Fig. 3. Influence of Pr fraction x on J_r (•), $_iH_c$ (Δ) and $(BH)_{max}$ (n) of nanophase $(Nd_{1-x}Pr_x)_{12}Fe_{82}B_6$ ribbons with d_g in the range 26-32 nm

CURIE TEMPERATURE ENHANCEMENT THROUGH Co SUBSTITUTION

The relatively low T_c for the $Nd_2Fe_{14}B$ phase (312°C) is a significant disadvantage of NdFeB magnets since it places severe limits on the maximum temperatures at which they can be operated. The problem is accentuated for nanophase alloys, and particularly nanocomposite alloys, since the room temperature $_iH_c$ is reduced considerably by the exchange coupling. There is a further reduction in thermal stability on substituting Nd by Pr because of the slightly lower T_c for $Pr_2Fe_{14}B$ (287°C) than for its Nd counterpart. Partial substitution of Fe by Co provides a useful method of compensating for the effects of the reduced $_iH_c$ at room temperature, though this inevitably increases the raw material cost. Also, it can negate the economic advantage that would otherwise be gained from employing nanocomposite alloys with reduced RE content.

The influence of Fe substitution by Co on T_c for the 2/14/1 phase in nanophase NdFeB [23], PrFeB [14] and $(Nd_{0.75}Pr_{0.25})FeB$ alloys [24] of near-stoichiometric composition is shown in Fig. 4 for varying ranges of Co concentrations. The effect on T_c of increasing Co substitution is linear in each case though the rate of increase for the Pr base alloy appears to be somewhat smaller than for the Nd base alloy. For a 20% Co substitution for Fe, for instance, the enhancement in T_c varies between ~165 K for PrFeB and ~185 K for NdFeB which provide the potential for very useful increases in thermal stability for the nanophase alloys. As would be expected, the absolute values of T_c for the Didymium base alloys are intermediate between those for Nd and Pr.

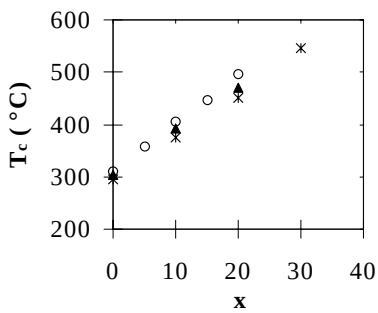

Fig. 4. Effect of Co substitution x for Fe on the Curie temperature T_c of $RE_{12}(Fe_{100-x}Co_x)_{82}B_6$ alloys for RE = Nd (o), = Pr (s) and = $Nd_{0.75}Pr_{0.25}$ (s)

MAGNETIC PROPERTIES OF NANOPHASE PrFeCoB ALLOYS PROCESSED BY OVERQUENCHING AND ANNEALING AND BY DIRECT QUENCHING

Most of the studies of exchange enhanced melt spun REFeB alloys have been undertaken on samples produced by direct quenching from the liquid to the nanocrystalline state at the highest cooling rates that still result in a completely crystalline structure (i.e. cooling rates that just avoid the initiation of vitrification [25]). Although this route is very effective in terms of minimising the scale of the grain structure it has the major disadvantage of giving a narrow process window and a limited degree of control which restricts its applicability for the bulk production of alloy ribbon for commercial magnets. A preferred route is to overquench the molten alloy into a fully amorphous state, followed by a devitrification anneal. Hence, in the quenching phase of the process, the processing parameters (mainly the roll velocity and the melt flow rate) are adjusted so that the cooling rate substantially exceeds the threshold value required for vitrification [26].

The magnetic properties of single phase, near-stoichiometric $Pr_{12}(Fe_{100-x}Co_x)_{82}B_6$ alloys (d_g = 35 – 45 nm), processed by direct quenching (DQ) [12] and by overquenching and annealing (OQA) [14] at 750°C for 5 mins, are compared in Fig. 5 for the range of Co substitutions x = 0 – 0%. Interestingly, in spite of d_g being nominally the same for the two series, the enhancement of J_r was greater for the OQA alloys when x < 20%. This is reflected in larger $(BH)_{max}$ for the OQA alloys when x ≤ 15% but $_iH_c$, in contrast, is systematically smaller for the whole range of x. The reason for the larger J_r enhancement for OQA than for DQ alloys in the lower x range may have been the result of a narrower distribution of 2/14/1 grain size. The smaller $_iH_c$ would be consistent with the larger J_r for x < 20% while the smaller $_iH_c$ for x > 20% may have reflected the effect of Co in decreasing H_A at higher concentrations. On the other hand, it is not clear why J_r decreases relatively rapidly beyond x = 20% for the OQA alloys, in spite of the nominally constant value of d_g.

These data indicate that very satisfactory combinations of exchange enhanced properties can be achieved by the preferred overquench/anneal route for the near-stoichiometric $Pr_{12}(Fe_{100-x}\ Co_x)_{82}B_6$ system when x ≤ 20%. For instance, for x = 10%, $(BH)_{max}$ ~220 kJm^{-3}, $_iH_c$ ~650 kA/m and T_c ~365°C. The excellent $(BH)_{max}$ value results from an especially square second quadrant J-H loop shape.

The magnetic properties of nanocomposite $Pr_{10}(Fe_{100-x}\ Co_x)_{84}B_6$ alloys (d_g = 35 – 50 nm) produced by the DQ [12] and OQA [14] routes, in the latter case annealed at 700 °C for 5 mins, are compared in Fig. 6 for the range of x = 0 – 40%. Except for x = 30% $_iH_c$, J_r and $(BH)_{max}$ for the OQA samples are consistently and substantially inferior to those of the DQ samples; even though J_r for the OQA are > 0.95 T for all x, only for the Co substitution x = 30% is $(BH)_{max}$ > 135 kJm^{-3}. It is significant that this is also the only composition for which $_iH_c$ for the OQA samples approaches that for their DQ counterparts. Thus, the disappointingly low $(BH)_{max}$ for all x ≠ 30% appears to be a combination of a poor second quadrant J-H loop shape and a low value of $_iH_c$, which lead to a non-linear B-H characteristic.

The generally poor properties for the OQA nanocomposite alloys is probably the result of simultaneous growth of grains of α-Fe and 2/14/1 phase in the low temperature regime. In crystallisation, during cooling from the liquid state (DQ), the α-Fe phase (and evidently, the 2/14/1 phase) nucleates very readily, leading to ultra-fine crystallites of mean diameter ~15 nm, partly reflecting the relatively low volume fraction (~15 vol % at 10% RE) of this phase. Thus, the whole of each α-Fe crystal (exchange length ~30 nm) would be expected to be exchange coupled to the adjacent 2/14/1 crystals. In the case of the OQA alloys, however, nucleation and growth of crystals takes place at much lower temperatures, corresponding to a regime of much smaller nucleation frequencies than for the DQ alloys. Thus, fewer but larger

α-Fe crystals would be expected in the former than in the latter. Evidence in support of this was obtained by TEM studies on these alloys [27] in which the OQA alloys tended to manifest a unimodal distribution of grain sizes centred at ~40 nm, in contrast to the DQ alloys which showed a clearly bimodal distribution with one peak centred at ~15 nm, corresponding to α-Fe, and another centred typically at ~40-45 nm, corresponding to the 2/14/1 grains. Such coarser α-Fe crystallites in the OQA samples may not be completely exchange coupled to the adjacent 2/14/1 grains and this could account for the inferior second quadrant loop shapes observed in those alloys. More rapid heating to a higher annealing temperature is one possible means of enhancing the nucleation frequency, especially of the α-Fe, and thus of overcoming this problem. Another option is to add small concentrations of refractory metal dopants such as Zr and/or Nb which are known to promote nucleation [14,15,28].

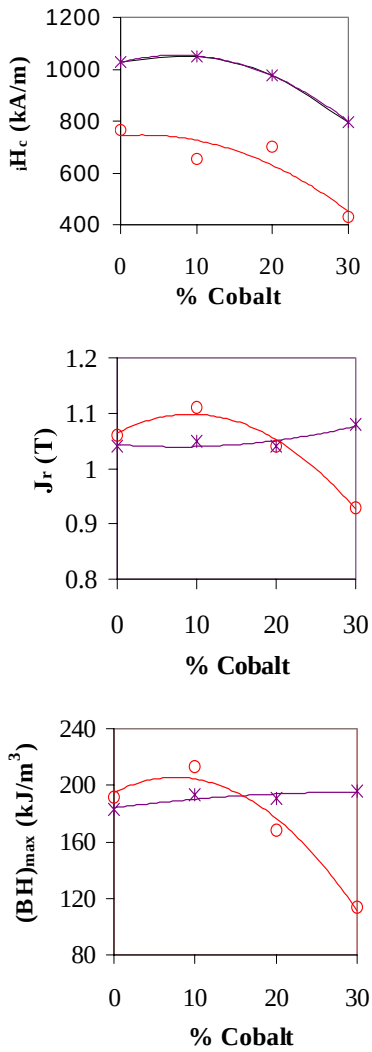

Fig. 5. $_iH_c$, J_r, and $(BH)_{max}$ as function of Co content x for single phase $Pr_{12}(Fe_{100-x}Co_x)_{82}B_6$ alloys: o- overquenched and annealed at 750 °C for 5 min; s directly quenched

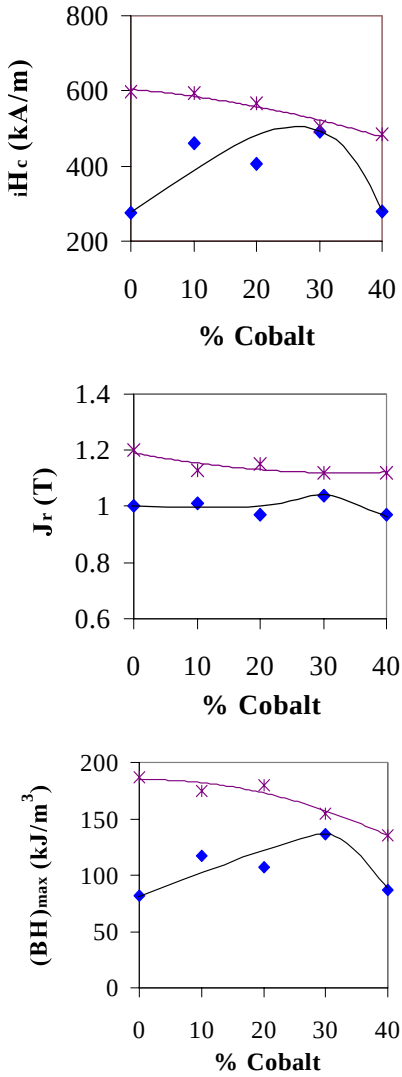

Fig. 6. $_iH_c$, J_r, and $(BH)_{max}$ as function of Co content x for composite $Pr_{10}(Fe_{100-x}Co_x)_{84}B_6$ alloys: u overquenched and annealed at 700 °C for 5 min; s directly quenched

INFLUENCE OF DOPANT ADDITION OF Zr ON MAGNETIC PROPERTIES

The magnetic properties of directly quenched nanophase $(Nd_{0.75}Pr_{0.25})_yFe_{94-y}B_6$ (d_g = 25-36 nm) [12] and $(Nd_{0.75}Pr_{0.25})_yFe_{93-y}Zr_1B_6$ (d_g = 22-28 nm) [15] alloys as a function of RE concentrations y are shown in Fig. 7. There is a clear grain refining effect (between 10 and 25 %, depending on RE:Fe ratio) associated with the 1 at % Zr substitution for Fe [15], as was also observed previously for nanophase PrFeB [28], presumably due to its effect on the nucleation and/or growth of the 2/14/1 phase. Nevertheless J_r is lower for the Zr-containing sub-stoichiometric alloys containing 8 and 10 at % RE, probably because of the decrease in J_s for the 2/14/1 phase [29] (although it might have been expected that J_r for the stoichiometric y = 12 alloy would also have

been adversely affected by this). The J_r enhancement for the RE-rich alloy (14 at % RE) resulting from the Zr addition is probably simply the result of the grain refining effect. $_iH_c$ is, in contrast to J_r, increased by the Zr addition over the range of RE contents from 8 to 12 at %, which is consistent with the reported increase in H_A [29]; for the RE-rich alloy, a slightly lower $_iH_c$ is induced by Zr. The behaviour of J_r and $_iH_c$ in this RE-rich alloy suggest that the Zr may be tending to enter the RE-rich phase preferentially. The larger $(BH)_{max}$ values on adding Zr for the 8-12 at % RE alloys, result from improved loop squareness and, for the low RE alloys, the larger $_iH_c$.

Fig. 7. Magnetic properties of directly quenched nanophase $(Nd_{0.75}Pr_{0.25})_yFe_{94-y}B_6$ (o) and $(Nd_{0.75}Pr_{0.25})_yFe_{93-y}Zr_1B_6$ (u)

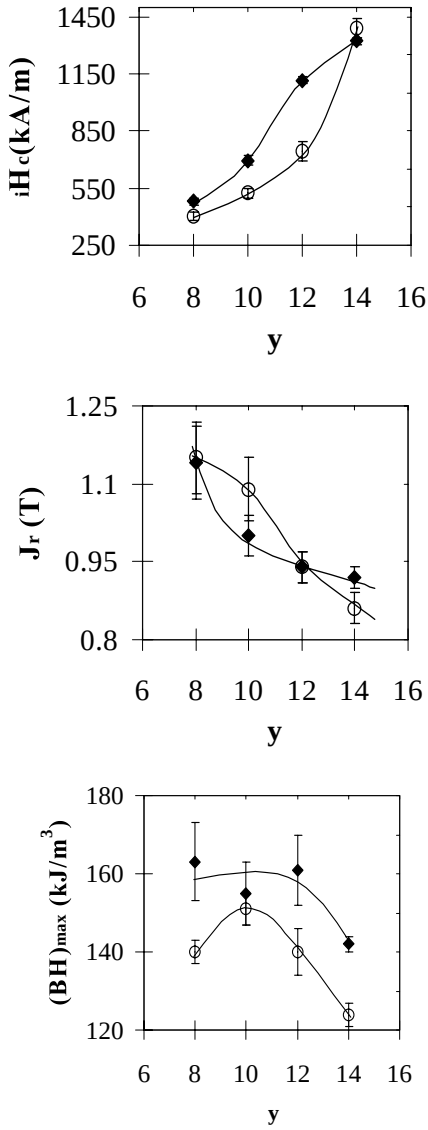

as function of RE content y

SUMMARY AND CONCLUSIONS

The coercivity $_iH_c$ of exchange enhanced, nanophase PrFeB alloys is larger than for corresponding NdFeB alloys of the same mean 2/14/1 grain size by approximately 20-30%, depending on the RE:Fe ratio, because of the larger anisotropy field for $Pr_2Fe_{14}B$ than for $Nd_2Fe_{14}B$. This is especially useful for low RE nanocomposite alloys, which have low $_iH_c$ in the case of NdFeB. Excellent combinations of $(BH)_{max}$, $_iH_c$ and Curie temperature T_c are attained by the overquench and anneal route for nanocrystalline single phase $Pr_{12}(FeCo)_{82}B_6$ alloys. However, only for 30% substitution of Fe by Co could acceptable enhancement of $(BH)_{max}$ be attained by this route for nanocomposite $Pr_{10}(FeCo)_{84}B_6$ alloys.

The coercivities of directly quenched nanophase Didymium (NdPr)-Fe-B alloys, with d_g ranging from 26-32 μm, are intermediate between those of the corresponding NdFeB and PrFeB alloys. The remanence J_r and maximum energy product $(BH)_{max}$ show maxima at a Nd:Pr ratio of 1:3.

Addition of 1 at % Zr gives a significant grain refinement and, combined with enhancement of the anisotropy field, leads to useful improvements in magnetic properties for most of the NdPrFeB alloys.

The influence of decreasing $RE_2Fe_{14}B$ grain size d_g on J_r and $_iH_c$ for nanocomposite NdPrFeB/α-Fe alloys is shown to be different for that of single phase alloys investigated earlier. As predicted from micromagnetic modelling the presence of sufficient soft phase results in both J_r and $_iH_c$ increasing with decreasing d_g.

REFERENCES

1. J. J. Croat, J. F. Herbst, R. W. Lee and F. E. Pinkerton, J. Appl. Phys., 55 (1984) 2078.
2. R. W. Lee, Appl. Phys. Lett., 46 (1985) 790.
3. E. C. Stoner and E.P. Wohlfarth, Phil. Trans. Roy. Soc., 240 (1948) 599.
4. R. W. McCallum, A. M. Kadin, G. B. Clemente and J. E. Keem, J. Appl. Phys., 61 (1987) 3577.
5. A. Manaf, R. A. Buckley, H. A. Davies and M. Leonowicz, J. Magn. Magn. Mater., 101 (1991) 360.
6. A. Manaf, R. A. Buckley and H. A. Davies, J. Magn. Magn. Mater., 128 (1993) 302.
7. A. Manaf, P. Z. Zhang, I. Ahmad, H. A. Davies and R. A. Buckley, IEEE Trans. Magn., 29 (1993), 2866.
8. H. A. Davies, J. Magn. Magn. Mater., 158(8) (1996) 11.
9. R. Coehoorn, D. B. de Mooij, J. P. W. B. Duchateau and K. H. J. Buschow, J. de Phys. Colloque C8, 1988, 49, C8-669.
10. J. Ding, P. G. McCormick and R. A. Street, J. Magn. Magn. Mater., 124 (1993) 1.
11. G. Mendoza-S and H. A. Davies, J.: *Alloys and Compounds*, 281 (1998) 17.
12. H. A. Davies, C. L. Harland, J. I. Betancourt R. and G. Mendoza, Proc. MRS Symp. on Advanced Hard and Soft Magnetic Materials. Eds. Michael Coey et al., Warrendale, USA, 1999, pp. 27.
13. J. I. Betancourt R. and H. A. Davies, J. Appl. Phys., 85 (1999) 5911.
14. C. L. Harland and H. A. Davies, J. Appl. Phys., 87 (2000) 6116.
15. J. I. Betancourt R. and H. A. Davies: Proc. 16th Intl. Wkshop. on RE Magnets and their Applications, eds H Kaneko et al, pp 595-604 (2000, Japan Inst Metals, Sendi).
16. H. A. Davies and J. I. Betancourt R.: Proc. 16th Intl. Wkshop. on RE Magnets and their Applications, eds H Kaneko et al, pp 485-494 (2000, Japan Inst Metals, Sendi).

17. C.L. Harland, H.A. Davies, B.E. Watts and F. Leccabue, Proc. 15th Int. Workshop on RE Magnets and their Applications. Eds. L. Schultz and K.H. Muller., MATINFO, Frankfurt, 1998, pp. 263
18. G.E. Carr, H. A. Davies and R.A. Buckley, Mater. Sci. Eng., 99 (1988) 147.
19. S. Hirosawa, Y. Matsuura, H. Yamamoto, S. Fujimura, M. Sawaga and H. Yamauchi, J. Appl. Phys., 59 (1986) 873.
20. T. Schrefl, J. Fidler and H. Kronmüller, Phys. Rev. B, 49 (1994) 6100.
21. P. Z. Zhang and H. A. Davies, Internal Report, Department of Engineering Materials, 1994.
22. R. Fischer, T. Schrefl, H. Kronmüller and J. Fidler, J. Magn. Magn. Mater., 153 (1996) 35.
23. R. Yapp and H.A. Davies, Proc. 14th Int.Workshop on Rare-Earth Magnets and their Applications., Ed. F.R. Missell et. al., World Scientific, Singapore, 1996, pp. 563.
24. J.I. Betancourt R. and H.A. Davies, to be published.
25. H.A. Davies, Phys. Chem. Glasses, 17 (1976) 159.
26. A. Jha, H. A. Davies and R. A. Buckley, J. Magn. Magn. Mater., 80 (1989)109.
27. C.L. Harland and H.A. Davies, to be published.
28. D. Goll and H. Kronmüller, Proc. 15th Int. Workshop on RE Magnets and their Applications, Eds. L. Schultz and K.H. Muller. MATINFO, Frankfurt, 1998, pp. 189.
29. M. Jurczyk and W.E. Wallace, J. Magn. Magn. Mater. 59 (1986) L182.

Acknowledgements

The financial support of the EPSRC through the Advanced Magnetics Programme is gratefully acknowledged. JIBR and CLH acknowledge the award of research scholarships by DGAPA, UNAM, Mexico and by the Department of Engineering Materials, University of Sheffield, respectively.